VIA MEDICA

Nuclear Medicine Review 2007
Vol. 10, No. 1, pp. 29–42

ISSN 1506–9680

Review

Cerebral hemodynamics and investigations of cerebral blood flow regulation

Wojciech Rudziński[1], Maciej Swiat[2], Maciej Tomaszewski[1], Jaroslaw Krejza[1, 3]

[1]Department of Radiology, Division of Neuroradiology of the University of Pennsylvania, United States
[2]Department of Neurology, Aging, Degenerative and Cerebrovascular Diseases, Medical University of Silesia, Katowice, Poland
[3]Department of Nuclear Medicine, Medical University of Gdansk, Poland

[Received 20 III 2007; Accepted 7 IV 2007]

Abstract

To maintain adequate cerebral blood flow despite frequent changes in systemic arterial blood pressure and to constantly adjust blood supply to the current metabolic demand dictated by neuronal electrical activity, brain developed a myriad of mechanisms. These are designed to protect central nervous system from fatal consequences of hypoxia and energy deficit and are collectively called "cerebral autoregulation". Despite years of research mechanisms responsible for regulation of CBF functioning under physiologic and pathologic conditions are still not clear. When these mechanisms are damaged or exhausted, patients life is in danger, as even slight, negligible under normal conditions, systemic hemodynamic disturbances might lead to cerebral infarct. Even perfect imaging of the irreversible brain damage with MR for the particular patient is too late action. Thus, detection of cerebral blood flow disturbances and impaired autoregulation, which are known to be associated with high risk of stroke, are extremely important in clinical practice. Several methods have been developed to quantify this process and thus evaluate risk of cerebral ischemia and guide therapeutic process. This review focuses on current knowledge on physiology of regulation of cerebral blood flow, mechanisms responsible for brain damage resulted from cerebral ischemia and reviews noninvasive diagnostic tests to assess cerebral autoregulation.

Key words: brain, cerebral circulation, cerebrovascular reactivity, autoregulation, hemodynamics

Correspondence to: Jaroslaw Krejza
Department of Radiology of the University of Pennsylvania
Division of Neuroradiology, Science Building ste 370
3600 Market street, Philadelphia, PA 19104, USA
e-mail: Jaroslaw.krejza@uphs.upenn.edu

Cerebral blood flow regulation

Brain tissue constantly maintains an extremely high metabolic rate. Cerebral oxygen consumption (≈ 3.5 ml/100g tissue/min) [1] accounts for about 20% resting total body oxygen consumption. The metabolic demand must be matched by high blood flow supply, which on average exceeds 50 ml/100g tissue/min, accounting for 15–20% of the total cardiac output [1, 2]. As the brain almost exclusively uses glucose for its energy metabolism and in general does not store energy, continuous blood supply, maintained within a narrow range, is absolutely required for brain function (90%) and cell viability (10%) [3]. Cerebral blood flow (CBF) is driven by cerebral perfusion pressure (CPP), represented by the difference between mean arterial blood pressure (ABP) and intracranial pressure (ICP), working in concert with cerebrovascular impedance. The components which make up cerebrovascular impedance include:

— cerebrovascular resistance (CVR), which is inversely proportional to the forth power of the vessel radius when laminar flow occurs and the flow is in steady state;
— the internal fluid resistance, which depends on viscoelastic properties of arterial walls, viscosity of the blood and flow velocity;
— the blood inductance, which is dependent on its rheostatic properties and momentum;
— the vascular compliance, which is related to the elasticity of the vessel wall [4, 5].

Alteration of any of the components, which make up impedance in a non steady-state system, such as occurs in the cerebrovascular system, can significantly impact the blood flow. Microvascular constriction, however, most significantly increases the impedance [6]. The ability of brain microvasculature to maintain cerebral blood flow relatively constant despite wide variations in CPP is called "cerebral autoregulation" (CA). In the normal state CA maintains relatively constant CBF within the range of mean ABP from about 60 to 150 mm Hg [7]. It should be mentioned, however, that upper and lower limits of CA are not fixed and can be shifted up or down by endogenous as well as exogenous factors. Sympathetic nervous system activity and increased levels of Angiotensin II, for example, shift upper and lower limits of CA up towards higher pressures, while chronic use of antihypertensive medications have opposite effects [8, 9]. Patients with untreated hypertension have limits of regulation set on higher level in com-

parison to healthy people [8]. This is important because in these patients overzealous antihypertensive treatment may lead to dangerous reduction of CBF at relatively high ABP. The mechanisms of CA are complex and not fully understood. It is surmised from the results of numerous experimental studies that CA is maintained by three different control pathways: vasogenic, metabolic and neurogenic.

The *vasogenic* mechanism is based on the intrinsic ability of cerebral vessels to respond to changes in shear stress and transluminal pressure [10]. Increase in transluminal pressure activates vascular smooth muscle cells leading to decrease in the diameter of arteries [11, 12]. On the other hand, contraction of cerebral vessels increases vascular wall shear stress [13]. This triggers endothelial cells to release factors, that relax vascular smooth muscles and dilates vessels [12]. These counteracting mechanisms assure optimal adjustment of the vessel diameter to CPP at any time.

The exact mechanisms of vascular contraction in response to increase in transluminal pressure remain unclear. It appears, however, that mechanical dilation of smooth muscle cells leads activation of phospholipase C (PLC) [14]. Increased PLC activity leads to elevated diacylglycerol levels, which activates protein kinase C, which is known to activate nonselective cation channels, depolarizing the smooth muscle membrane potential and enhancing calcium entry through voltage-dependent calcium channels. Increased concentration of free calcium ions activates the myosin light chain kinase, which phosphorylates myosin light chains and causes muscle contraction [15]. It is also possible that stretch of muscle cells directly activates calcium channels and leads to increased calcium concentration without activation of PLC- dependent pathway [16]. In contrary to intraluminal pressure-induced contraction, which seems to be dependent only on smooth muscle cells, shear stress-induced vasodilatation requires interaction of endothelial cells and vascular muscles. Synthesis of nitric oxide (NO) is necessary for this phenomenon to occur [17]. Shear stress increases activity of endothelial nitric synthase (eNOS) and causes release of NO, which diffuses to adjacent smooth muscle cells and induces vasodilatation through activation of potassium channels in those cells [18, 19]. Shear stress may also directly increase expression of eNOS as a shear stress-response element has been found in promoter region of gene for eNOS [20]. It is not clear, how significant a role the vasogenic mechanism plays in maintaining and regulation CBF and whether it depends somehow on caliber of the involved cerebral arteries.

In *metabolic* regulation, arterial resistance is modified by waste products of energy metabolism (CO_2), partial pressure of O_2, and release of specific vasoactive substances such as adenosine and potassium ions from neurons in response to insufficient blood supply. The most important metabolic factor is tension of CO_2 in periarteriolar space, although CVR is not directly affected by the CO_2 tension. It is the accompanying shift in periarteriolar pH, which regulates diameter of cerebral vessels [21]. Hypercapnia and the resulting decrease in extracellular pH causes cerebral vasodilatation and increase in CBF, while hypocapnia leads to cerebral vasoconstriction and CBF decrease. Mechanisms responsible for regulation of CVR by CO_2 tension and accompanying pH changes are not clear. Hydrogen ions may directly activate potassium channels in smooth muscle cells leading to its hyperpolarization or they may induce release of vasodilatory prostaglandins, adenosine or NO from neurons, glia or vessels [22–26]. Hypoxia, potassium ions and adenosine also lead to hyperpolarization of smooth muscle cells and consequently dilation of cerebral vessels. It appears that hypoxia-induced vasodilatation is mediated by activation of potassium channels, while increased concentration of potassium ions in extracellular fluid activates electrogenic Na/K pumps and smooth muscle inward rectifier potassium channels [27, 28]. Adenosine acts on cerebral vessels through its receptors located in arterial smooth muscle membrane [29]. Activation of these receptors leads to opening of calcium-dependent and ATP-dependent potassium channels [30, 31].

While there is a consensus that vasogenic and metabolic mechanisms play critical role in regulation of cerebrovascular tone, the importance of *neurogenic* regulation in the control of CBF is still a matter of debate. The cerebral vessels are innervated by extrinsic and intrinsic systems of nerve fibers. The “extrinsic” system refers to nerve fibers originating in ganglia belonging to sympathetic, parasympathetic and sensory ganglia, while nerves originating within the brain represent an "intrinsic" system [32]. Activation of sympathetic vascular nerves leads mainly to release of norepinephrine and neuropeptide Y [33]. Sympathetic stimulation constricts large cerebral arteries. However, CBF does not decrease, because the constriction of large cerebral vessels is immediately compensated for by dilation of resistance arterioles [34]. The role of sympathetic innervation seems to be related to protecting the brain against ABP increases through the mechanism of sympathetic activation shifting the upper and lower limits of CA towards higher pressures. Parasympathetic vascular nerve fibers release vasoactive intestinal polypeptide, acetylcholine and NO [35, 36]. Activation of these nerves causes cerebrovascular dilation, the physiological significance of which is still not clear [37]. Fibers originating in sensory ganglia contain clacitonin gene-related peptide, substance P, neurokinin A and pituitary adenylate cyclase-activating polypeptide [38–40]. These fibers cause dilatation of cerebral vessels and their physiological role appears to be counteracting action of cerebral vasoconstrictors [41]. Activation of these fibers may contribute to increase in CBF occurring in pathologic conditions such as meningitis and may play a role in pathogenesis of migraine [42, 43].

Vascular fibers belonging to the intrinsic system originate in different parts of brain such as nucleus basalis, locus coeruleus and raphe nucleus [44–46]. These fibers may modulate vascular tone directly or through stimulation of perivascular interneurons and glial cells [47, 48]. Activity of the intrinsic system may decrease or increase local blood flow depending on the rostrocaudal level of activation of their cells of origin within the brain. The physiological significance of this system is not yet completely elucidated [45, 46].

For academic purposes, CBF regulation is parceled into several major mechanisms, though the division is somehow artificial. The mechanisms influence and modify each other at any given time and the overall cerebrovascular tone is the product of interplay of many processes. It is clear that some of these mechanisms share common biochemical pathway at the level of vascular muscle cells. For instance vascular dilation caused by parasympathetic activation, shear stress and hypercapnia, at least in part, are mediated by the same factor — NO [49].

Neurovascular coupling in humans

The brain's information-processing capacity is limited by the amount of oxygen and energy available. When neurons are active, blood flow in that local brain region increases to meet the enhanced local metabolic demand [50]. The tight coupling between neuronal activity and blood flow is known as the "neurovascular coupling". This phenomenon seems to be dependent on both astrocytes and perivascular neurons.

Increased local neural activity leads to release of glutamate acting on astrocytic metabotropic glutamate receptors [51]. Activation of glutamatate astrocytic receptors leads to increased synthesis of arachidonic acid, which is metabolized to vasodilatory prostanoids like Prostalgandin E2 (PGE2) and epoxyeicosotrienoic acid (EET) [52, 53]. PGE2 and EET diffuse to vascular muscle cells and dilate vessels increasing local blood flow [52, 53]. However, during this process significant amount of arachidonic reaches vascular muscles as well. Smooth muscle cells contain enzymes (CYP4A), which generate powerful vasoconstrictor 20-hydroxyeicosotetraenoic acid (20-HETE) counteracting PGE2 and EET — induced vasodilatation [48, 54]. The question arises, what shifts this balance towards vasodilatation? Glutamate released into synaptic space activates postsynaptic NMDA-type glutamate receptors located on perivascular neurons [55, 56]. This leads to activation of neuronal NO synthase and production of NO, which reaches smooth muscle cells. NO not only exerts vasodilatory effects but also binds to the heme moiety of CYP4A enzyme and inactivates it, thereby preventing further synthesis of 20-HETE from arachidonic acid [57, 58]. Thus activation of both nNOS positive neurons and astrocytes seems to be necessary for proper functioning of neurovascular coupling. It is likely that astrocyte-derived vasodilatory prostanoids are direct mediators while neuronal NO acts as a modulator of this process.

Respiratory and cardiovascular factors and cerebral hemodynamics

Both oxygen and CO_2 tension have powerful effects on cardiovascular system through the peripheral and central chemoreceptors. Peripheral chemoreceptors are located in the aorta and internal carotid artery and respond to both hypoxemia and hypercapnia. The peripheral chemoreflex causes hyperventilation, transiently activates sympathetic traffic to peripheral blood vessels, and increases vagal activity to the heart [59]. Activation of peripheral chemoreceptors does not change CBF [60]. Central chemoreceptors are located in ventrolateral medulla and detect pH changes of the interstitial fluid [61]. Activation of the central chemoreceptor reflex causes hyperventilation and increased sympathetic stimulation to vasculature. Changes in sympathetic tone have a limited effect on CBF at normal $PaCO_2$ levels [62]. However, the sympathetic nervous system seems to attenuate the CO_2-induced increase in CBF. This phenomenon may indicate a moderate direct effect of the sympathetic nervous system on the cerebral vasculature [62]. Sympathetic stimulation can have more important effects on segmental vascular resistance and cerebral microvascular pressure in pathologic conditions. Generalized increases in the sympathetic discharge, causing substantial increases in ABP, can prevent concomitant increases in CBF by acting on both small resistance and large vessels [34, 63].

Arterial baroreceptor reflex, which plays an integral role in regulating peripheral vascular tone and heart rate in response to changes in ABP, seems to have no impact on the CBF. Neither interruption nor stimulation of baroreceptor nerves affects CBF or CVR at ABP within the range of CA [64, 65]. However, cerebral vasoconstriction occurs in healthy humans during graded reductions in central blood volume. The magnitude of this response is small compared with changes in systemic vascular resistance [66]. It seems that this degree of cerebral vasoconstriction is not by itself sufficient to cause syncope during orthostatic stress, but can exacerbate the decrease in CBF associated with hypotension if hemodynamic instability develops.

Cerebral ischemia and investigations of cerebral blood flow regulation

Cerebral infarction results when blood supply is not sufficient to support cellular viability or when low nutrients supply induces apoptosis. The cell death is a complex function resulting from a combination of the duration and magnitude of ischemia, the nutrients and oxygen content of blood, the specific cerebral structure involved, and ability of the tissue to dissipate the metabolic heat. Cell viability may be lost in as little as 20 minutes after cessation of blood flow. In mild but prolonged low perfusion states, irreversible gray matter damage will occur with CBF below approximately 20 mL/100 mg/h. Figures 1–4 demonstrate a basic concept of chain reactions in neuron and glia cells under different ischemic conditions, which eventually lead to cell death.

In general, ischemia results from:

— sudden arterial occlusion;
— global hypoxia due to respiratory or cardiac arrest;
— hypoperfusion in patients with high ICP;
— subacute or chronic borderline hypoperfusion due to occlusion or narrowing of large cerebral arteries. The last two need more explanation.

Cerebral blood flow disturbances in patients with high ICP

According to the Monro-Kellie hypothesis [67] the cranium acts as a near rigid container of virtually incompressible substances such as brain (80%), blood (12%) and cerebrospinal fluid (CSF) — (8%). These three volumes completely fill the intracranial cavity and remain in a state of dynamic equilibrium with each other. Based on these premises, any extra volume added to the intracranial cavity will increase ICP. However, cessation of cardiac action leads to equalization of ICP with atmospheric pressure, no matter how high it was before stoppage of cerebral circulation. In other words, it will always equal zero when heart does not beat. Thus, it goes without saying that ICP is closely related to the function of cardiovascular system. Under normal CPP (80–100 mm Hg), ICP is not higher than 15 mm Hg [68]. Blood pressure in the cerebral arteries decreases as arterial diameter gets smaller and approaches the interstitial tissue pressure, that is equal to ICP at the level of brain capillaries and veins. The most significant drop in ABP occurs in small resistance, and precapillary arterioles. High ABP inside the arterial system is not transmitted to the brain tissue because it is confined within the arteries by thick arterial walls. More-

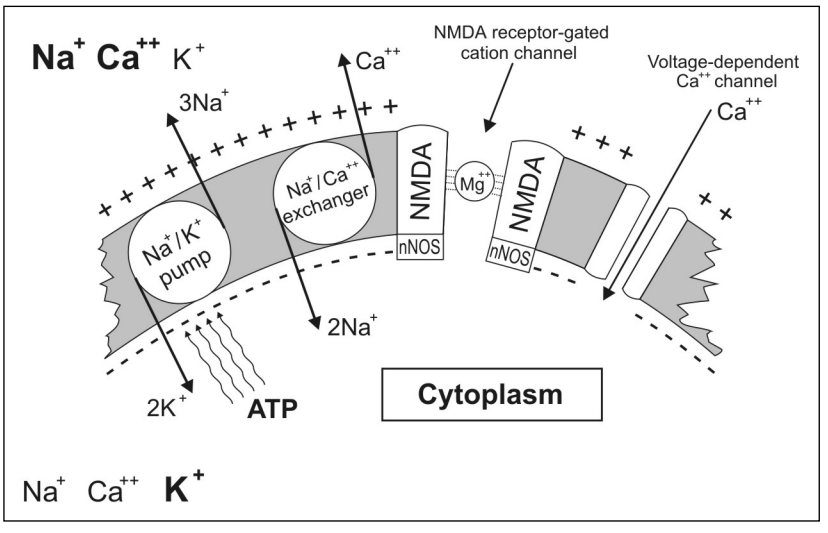

Figure 1. Physiological mechanisms of ion equilibrium in the neuron. The energy of in-flowing sodium ions is utilized for expelling the ions of calcium. Sodium is then removed by the Na\K pump. Negative potential of the cell interior helps keep the NMDA-coupled calcium channel locked with the ions of magnesium and inhibits the voltage-dependent calcium channels. nNOS — neuronal nitric oxide synthase, NMDA — glutamate (N-methyl-D-spartate) receptor, ATP — adenosinotriphosphate.

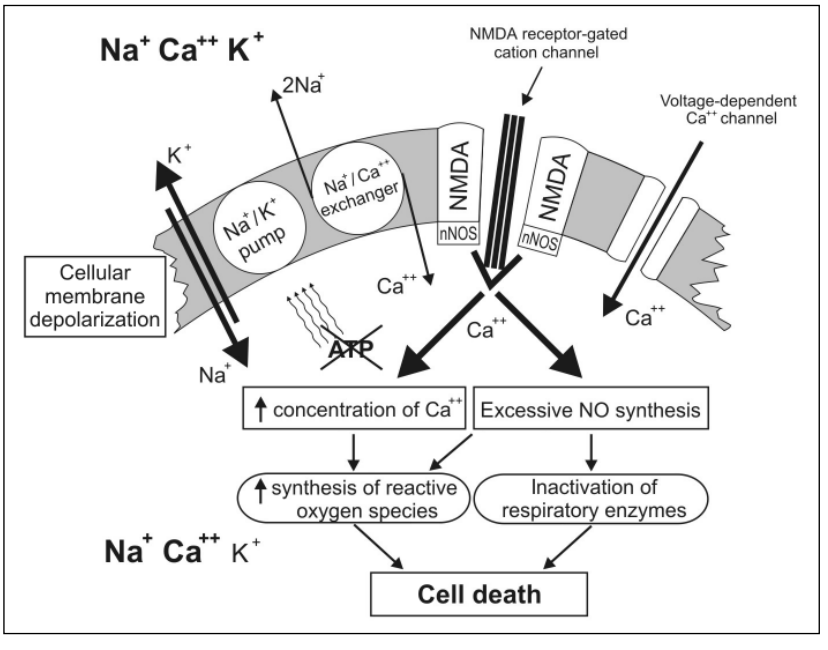

Figure 2. Ischemia and consequent energy deficit cause depolarization of the cell membrane, reverses the action of the sodium-calcium exchanger and allow influx of sodium and calcium ions into the cell. Depolarization opens the voltage-dependent calcium channels and releases magnesium-dependent block of NMDA-coupled calcium channel. The latter is made patent by glutamate, thus leading to increased synthesis of nitric oxide. Excessive concentration of nitric oxide and calcium leads to cell death.

over, during every cardiac systole, some CSF and venous blood is pushed out of the cranium to accommodate "cerebral" portion of stroke volume. Thus, under normal conditions, cranial cavity exhibits some compliance and there is only slight rise in ICP due to distention of cerebral arteries during cardiac systole.

As mentioned before, any extra space occupying by intracranial lesion is at the cost of the volume of other intracranial components in order to maintain the ICP at normal levels. Thus, during growth of tumors or the development of hematoma, CSF is absorbed and venous blood is pushed out of the cerebral veins to accommodate the volume of the abnormal lesion inside the skull. When these compensatory mechanisms are exhausted, ICP increases logarithmically as pathologic volume further increases [69]. As ICP increases, the CPP and consequently CBF begin to decrease. From then on, the highest priority is maintaining CBF, even at the price of further increase in ICP, as neural tissue is much

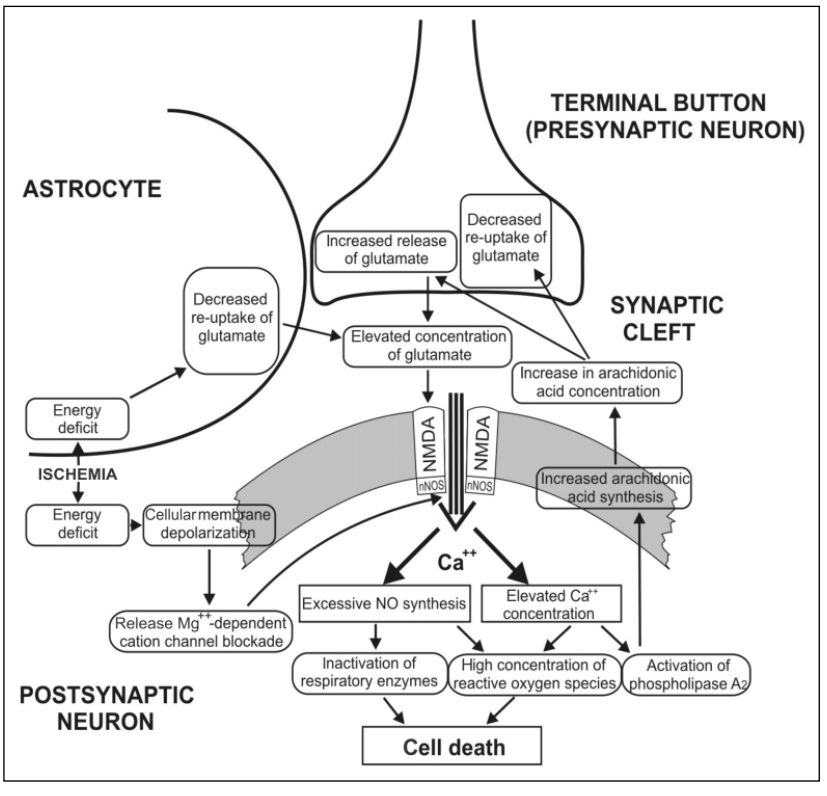

Figure 3. Biochemical mechanism of excitotoxicity. Energy deficit attenuates re-uptake of glutamate in the synaptic cleft. Increased content of this mediator causes overstimulation of NMDA receptor, excessive synthesis of nitric oxide and influx of calcium into the cell. This leads to inactivation of mitochondrial enzymes, free radicals production and activation of Phospholipase A2. The phospholipase releases arachidonic acid which again attenuates re-uptake of glutamate, thus producing the vicious circle of excitotoxicity.

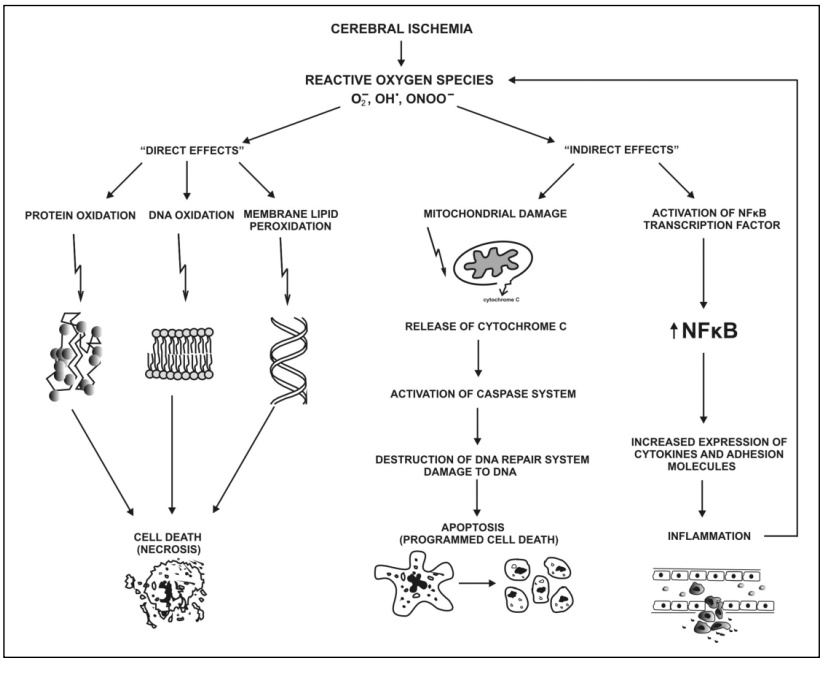

Figure 4. "Direct" and "indirect" effects of reactive oxygen species (ROS). Reactive oxygen species directly interact with DNA, proteins and lipids and destroy them through oxidation process causing cell death (direct effect). High concentration of ROS damage structure and function of mitochondria and change the redox state of the cell interior (indirect effect). Damage to the mitochondria leads to release of factors initiating process of programmed cell death (apoptosis). Oxidative stress activates transcription factor NFκB (nuclear factor κB), which induce synthesis many proinflammatory cytokines and adhesion molecules. Increased expression of cytokines and adhesion molecules augments inflammatory process in neural tissue.

more sensitive to ischemia than to pressure. It has been shown that neurons can withstand pressure several times higher than the atmospheric pressure [70].

Decrease in CPP lowers intraluminal ABP and leads to dilatation of arteries through the vasogenic mechanism. Furthermore, excessive buildup of CO_2, potassium ions, and adenosine add to the effect of hypoxia resulting from insufficient CBF to cause vasodilatation. Unfortunately, at this point, even significant vasodilatation does not help much improving CBF. Increased ICP constricts cerebral veins and is transmitted through their thin, compliant walls so that the point of maximal resistance of cerebral vascular bed shifts from arterial to venous system [71]. In other words, CBF decreases because of a lower and lower pressure gradient between arterial and venous system. High pressure in venous system decreases venous outflow and leads to congestive brain swelling.

Under these conditions, general cerebral vasodilatation has even more deleterious effects. Dilated arteries contain more blood and increased cerebral blood volume further increases ICP. Moreover, maximal arterial dilatation profoundly decreases stiffness of arterial walls, which become good transmitters of intraluminal ABP into the brain parenchyma [70]. Thus, increased cerebral blood volume, the transmission of intraluminal ABP into brain parenchyma, as well as decreased venous outflow are main determinants of ICP increase. In this situation, the dynamic system consisting of intracranial cavity and its contents loses its compliance and becomes "stiff" so that even small additional volume of systolic blood surge leads to huge ICP increase [72]. When ICP reaches the level of ABP, CPP decreases to zero leading to complete cessation of CBF. It will restart only if ABP rises sufficiently beyond the ICP to restore CBF. If this fails to occur, brain death occurs.

When the homodynamic disturbances caused by pathologic intracranial volume overcome physiologic mechanisms of intracranial volume compensation, ICP not only increases but also random ICP fluctuations begin to occur more frequently. Statistical analysis of these fluctuations has allowed pattern descriptions specific for increased ICP [73, 74]. These fluctuations are called A waves of Lundberg. A waves are characterized by a rapid rise in ICP up to 50–100 mmHg which is followed by a variable period during which the ICP remains elevated and then a rapid fall to baseline. These waves are also called "plateau" waves. It should be mentioned that when A waves occur, the baseline level of ICP is already elevated. Plateau waves develop as a result of a rapid increase in intracerebral blood volume, when sudden decreases in CPP leads to vasodilatation. Thus, plateau waves occur in patients with intact CA and reduced intracranial compliance. These sudden transient drops in CPP may be triggered by many, often poorly characterized factors. A well known trigger of A waves is postural change. The increase in CPP required to abort plateau waves may be generated by the Cushing phenomenon, which is activated when brainstem ischemia triggers systemic hypertension, thus increasing CPP [75]. During plateau waves, patients may have severe headache, visual disturbances, impairment of postural or motor control, altered consciousness, bradycardia and high ABP. The last two symptoms are caused by activation of Cushing reflex in effort to preserve CBF. However, in many patients plateau waves may not cause these symptoms and brain stem herniation ensues with minimal warning signs.

Based on these facts three very important conclusions should be drawn which are relevant for clinical practice. First, there is no perfect relation between clinical signs and severity of intracranial hypertension; second, monitoring of ICP is extremely important to gauge the risk of herniation; and third, maintaining CBF is the highest priority measure to treat patients with intracranial hypertension. Thus, close monitoring of CBF is extremely important when taking care of patients with intracranial pathology.

Chronic hypoperfusion and investigations of cerebral blood flow regulation

In patients with impaired CA even slight fluctuations in ABP may lead to cerebral ischemia or encephalopathy due to global or local hyperperfusion [76]. In such patients ischemia is the result of a combination of chronic and acute factors. Typically slowly progressive narrowing of the large cerebral artery leads to drop in local CPP. The perfusion deficit is most marked at the regions farthest from the main supplying arteries — the arterial border zones [76] — at the margins of the territories supplied by the anterior, middle, and posterior cerebral arteries or between the cortical vessels and small penetrating arteries at the base of the brain. The baseline drop in CPP makes these areas susceptible to fluctuations in systemic ABP, oxygen supply, and local vascular resistance. When the drop in perfusion is of short of duration, transient neurological deficits may occur, but when the CPP falls below critical levels for a sufficient duration, infarction will result. Thus, it is important to know in advance whether a patient is at high or low risk of brain infarct caused by hypoperfusion alone.

In disease states, produced for instance by marked arterial narrowing, the peripheral microvessels are maximally dilated, and a decrease in CPP results in a decrease of CBF. With mild decreases in CPP, cellular function is maintained by increased oxygen and nutrient extraction (called often as stage II) [77]. As CPP falls further, oxygen extraction reaches a maximum, and any decrease in CBF are accompanied by decreased oxygen consumption (referred to as "stage III"). When critical levels of oxygen and nutrient delivery cannot be met, cell death occurs.

Two main approaches to predict the risk of cerebral infarction due to drop of CPP are employed. One is to make quantitative measurements of oxygen extraction, oxygen consumption and CBF. In practice, such measurements can be made using positron emission tomography (PET) with $^{15}O_2$ and $C^{15}O_2$. An area with exhausted cerebrovascular reserve will show relatively decreased CBF and increased fractional oxygen extraction. Other methods of assessment of CA on the basis of measurements of oxygen extraction rate include arterio-venous O_2 difference and near-infrared spectroscopy. The second most often used approach is to measure the response of local CBF to a physiology challenge, such as pharmacologic vasodilatation, elevated CO_2 level, and a challenge with decreased ABP.

Perfusion imaging becomes a standard part of stroke imaging to determine the ischemic penumbra in patients with ischemic stroke. In case of chronic perfusion impairment, however, a single CBF or blood volume measurement is rather not adequate. First, interpretation of any single perfusion measurements is difficult because of the high physiological variability of CBF. Second, the relationship between absolute CBF and progression to infarction varies widely between and within patients. This is particularly im-

portant in assessing chronic rather the acute hypoperfusion, because the degree of flow decrement is generally of the same order as that from the physiological sources of variability [78]. Third, absolute perfusion measurements can be inaccurate because the models used to derive CBF are not sufficiently accurate. This problem is most significant in methods that depend on intravascular tracers. With these methods, a perfusion value is assigned from model-dependent calculations based on the dispersion of a tracer [79]. Regional perfusion, however, is only one of the factors that can affect this dispersion. An additional important factor is intravascular dispersion arising from convection and diffusion during bulk flow in the large arteries between the heart and the capillaries. This intravascular dispersion may vary substantially and depend on the degree of turbulence within the vessels and on the path length to the tissue of interest. Because this dispersion has effects on the tissue concentration versus time function that are similar to variation from capillary flow, variation in turbulence or path length will produce artifactual changes in the value obtained for tissue perfusion. Despite of these limitations assessment of absolute CBF is important, because an absolute decrease in CBF may help to identify the "steal" phenomenon.

The assessment of CA is free of the above mentioned limitations. It can be evaluated by measuring relative blood flow changes in response to the change in the blood pressure using "static" or "dynamic" approaches [80]. Both approaches attempt to establish whether CA is normal or impaired, using the autoregulatory curve of CBF in humans as a model [81, 82]. In the static method, evaluation of CA is performed under steady-state conditions. That is, a first measurement of CBF obtained at a constant baseline ABP is followed by another steady-state measurement that is taken after the autoregulatory response to a change in ABP has been completed. If the change in ABP (within the lower and upper limits of CA estimated for healthy humans) does not change CBF, CA is functioning properly. If manipulation of ABP evokes significant changes in CBF, the CA is impaired. In the static method, manipulation of ABP is usually achieved using vasoactive drugs. Static methods evaluate the efficiency of the CA, that is overall change in cerebrovascular impedance induced by changes in ABP.

Dynamic methods use rapid changes in ABP and analyze CBF and ABP during the whole autoregulatory process [80]. Systemic hemodynamic changes may be induced using rapid leg cuff deflation, progressive lower body negative pressure, Valsalva maneuver, deep breathing, ergometric exercise or head-down tilting. Dynamic methods are able to assess both efficiency and latency of CA response, that is overall change in CVR as well as the time in which the change in the CVR is achieved.

The use of systemic hypotension to challenge the CA response is limited, however, because pharmacologically induced hypotension could result in permanent ischemic injury, in particular in patients with already insufficient CBF. Balloon test occlusion itself is a focal challenge to CPP; but it is rather more important to know whether current flow is adequate than in the effect of complete occlusion. What is needed is a mild global challenge to cerebral perfusion that is unlikely to produce ischemia. Two methods of physiological challenge that meet these criteria and that have received substantial study for testing CA include a test with administration of acetazolamide and systemic partial CO_2 pressure manipulations.

Acetazolamide is a carbonic anhydrase inhibitor that acts as a potent cerebral vasodilator. Administered intravenously, it slowly penetrates the blood-brain barrier, where it reversibly inhibits the carbonic anhydrase in brain parenchyma. Carbonic anhydraze catalyzes the conversion of bicarbonate and hydrogen ion to water and CO_2. Acetazolamide decreases the production of bicarbonate and results in a decrease in the extracellular pH in the brain [83, 84]. This induced acidosis results in vasodilatation of small arterioles [85, 86]. Acetazolamide administration thus induces a considerable increase in CBF [86]. Doses used in the assessment of cerebrovascular reserve are in the 15–18 mg/kg range; in many studies a standard total dose of 1 g is used [87]. Systemic ABP, HR and respiratory rate are unaffected [88]. The effect on CBF may be seen within the first 5 minutes after administration, and steal phenomenon is most conspicuous at about 5 minutes [89]. Peak CBF augmentation occurs at approximately 10 minutes after bolus intravenous administration and diminishes little over the next 20 minutes. With these dose parameters, a 30% to 60% increase in CBF is achieved in normal subjects [90]. This response is little diminished in the healthy aged population [91]. The percentage increase in CBF after acetazolamide administration may be used to define cerebrovascular reserve based on the following formula:

$$\textit{Cerebrovascular reserve} = (CBF_{post} - CBF_{pre})/CBF_{preacetazolamide}$$

Although a global increase in CBF by about 30% is accepted as normal, a variety of criteria have been used to define an abnormal response to acetazolamide. The definition has varied among the major studies in which it was used, including such criteria as greater than 5% decrement in absolute CBF, a less than 10% increment in absolute CBF, an absolute change of less than 10 mL/ /100 g/min, and a value greater than two standard deviations below control values.

The bolus administration of acetazolamide over several minutes at these doses is generally well tolerated. The most commonly reported side effects of intravenous administration include transient perioral numbness, paresthesias, and headaches [88]. The theoretic concern of induced ischemia as results of the "steal" phenomenon has not been borne out by clinical experience [90].

Manipulation of arterial CO_2 tension ($PaCO_2$) has also been used to test cerebrovascular reserve. Low level hypercarbia results in a reproducible increase in CBF of 0.01–0.02 mL/g/min for each 1 mm Hg rise in $PaCO_2$. The effect is rapid and quickly reversible. It is mediated through a change in extracellular pH as well as NO and cyclic guanosine monophosphate and results from changes in vascular smooth muscle tone [92]. CO_2 manipulation has been performed with a number of schemes, including breath holding or hyperventilation, rebreathing, and inhalation of 3% to 5% CO_2. The effect of altered CO_2 tension on CBF has been quantified either as a fixed effect for particular CO_2 manipulation (similar to the quantification of acetazolamide effect) or as the slope of the CO_2 — CBF relationship according to the formula [93]:

$$\textit{Cerebrovascular reserve} = [(CBF_{post\text{-}CO2} - CBF_{pre\text{-}CO2})/ /(CBF_{pre\text{-}CO2})] \times [100/(P\alpha_{pre\text{-}CO2} - P\alpha_{post\text{-}CO2})]$$

In clinical practice, the magnitude of CBF changes is smaller

than that achieved with acetazolamide. The average increase in cerebrovascular reserve (percentage change in blood flow per mm Hg change in $PaCO_2$) is 1.1% to 2.9%. With 5% CO_2 inhalation, the CBF response is approximately half of the response to acetazolamide. Furthermore, although CO_2 manipulation and acetazolamide in theory both produce vasodilatation and alter CBF in similar fashion, the correlation between CBF changes produced by the two has varied from poor to moderate [94–96]. CO2 manipulation also has the disadvantage of itself altering systemic ABP — mean ABP increase of about 10 mm Hg with 5% CO_2 — an effect that may blunt the CBF response [94]. However, CO_2 manipulation is easily performed, generally well tolerated, and has no long-term effects. The rapid response to CO_2 makes it particularly suitable for transcranial Doppler (TCD) measurements.

An important phenomenon affecting the results of CA testing is that of "steal". In regions under stage II or III conditions, it is common to observe a decrease in CBF after vasodilator administration [90, 97]. This phenomenon is created by the interaction between regions of different cerebrovascular response and the systemic effects of the agents used for physiologic or pharmacologic challenge. Areas with proper CA will show vasodilatation, lowering the pressure in the larger blood vessels supplying both normal and abnormal areas. This lower pressure results in a drop in blood flow in the regions that are already maximally dilated.

In assessment of CA spatial and temporal resolution (the degree of CA impairment can be regionally and tissue specific), simultaneous imaging of parenchymal and vascular structures (status of parenchyma and large arteries is important in interpretation of autoregulatory test's results), invasiveness, cost and availability should be taken into account when one selects a testing technique.

Physiological techniques to assess functionality of CA

Physiological techniques include TCD, perfusion CT (pCT) and MR (pMR) imaging with dynamic contrast bolus administration, arterial spin-labeling MR perfusion (ASL MR), blood oxygenation level-dependent MR imaging (BOLD). More invasive techniques such as positron emission tomography (PET), single-photon emission CT, and Xenon CT are not reviewed here.

Transcranial Doppler ultrasonography (TCD)

The most popular technique used to assess CA using both static and dynamic methods is the measurement of blood flow velocity (CBFV) changes in cerebral arteries with TCD. Implementation of this technique is based on the fact that changes in CBF will be reflected by changes in CBFV. If CA is intact, drop or increase in ABP will not affect CBFV. This is because any change in ABP will be compensated by adequate change in diameter of small resistance arterioles. Thus, CPP, CBF and CBFV will remain unaffected.

Many investigators tried to formulate objective criteria to classify CA usually as normal/impaired using different approaches. For static methods, most commonly used measures of CA are correlation coefficient (*r*) between CBF and mean ABP as well as "index of static autoregulation" (*aARi*), which is expressed as a ratio of percentage change in CVR to percentage change in ABP (*sARi* = %CVR/%ABP) [98, 80]. The percentage change in CVR is calculated as the ratio of ABP to CBF (CVR = ABP/CBF). For perfect CA, correlation coefficient would equal 0 and aARi would be 1, while complete lack of CA would yield *r* and *sARi* of 1 and 0, respectively. Most commonly proposed threshold between normal and impaired CA for both r and s*ARi* is 0.5 [98, 99]. Evaluation of CA in dynamic methods is based on "dynamic CA index" (*dARi*). This is the dynamic equivalent of *sARi* and is defined as $dARi = (\Delta CVR/\Delta T)/\Delta ABP$, where ΔT is the time when CA response occurs [100, 80]. Thus, the dynamic CA index evaluates not only overall change in CBF induced by change in ABP, but also quantifies time-dependence of the CA response. A value of $dARi = 0$ represents the absence of CA, while value = 9 corresponds to a very efficient CA response. The proposed threshold value between normal and impaired CA is about 5 [80, 101]. Static and dynamic methods of evaluation of CA yield similar results [80].

TCD can only measure velocities in large arteries. Regional areas of impaired CA in an artery distribution may be missed when averaged with areas that are better perfused. Furthermore, correlation between flow velocities and CBF is weak in some patients, mostly because of collateral circulation [102, 103]. Also, TCD can not be performed in some patients due to absence of acoustic windows [104].

Perfusion CT and MR imaging with dynamic contrast bolus administration

The use of this technology for acute stroke evaluation is increasing. The bolus is tracked during the passage through cerebral circulation in order to calculate cerebral blood volume and CBF using models that are less robust than those used for freely diffusible tracers [105, 106]. In assessment of CA, however, this problem is minimized as preacetazolamide study serves as a control for postacetazolamide study, both can be performed at one session. The spatial resolution is high and the flow data can be easily mapped to the anatomic images. Furthermore, MR or CT angiography can be performed at the same time. The radiation dose, limited coverage of the brain and allergic reaction for contrast are disadvantages of the CT perfusion, whereas in MR perfusion is difficult to obtain reliable absolute quantitation because of the complex relationship between concentration and signal. CT perfusion has received limited but promising use in assessment of CA [107, 108]. The experience with MR perfusion is more extensive and promising [109, 110].

Arterial spin-labeling MR perfusion (ASL MR)

Experience with this method in evaluation of CA is limited. The effect of magnetic saturation or inversion of the protons in arterial blood on the MR signal is used to derive quantitative CBF measurements. This technique does not require exogenous contrast and provides good spatial resolution and repeatability. However, signal-to-noise ratio is poor, and imaging times of 3-6 minutes have been needed to obtain satisfactory results for even single-slice imaging. Though water is a diffusible tracer, the arterial transit time and limited diffusibility of water have effects on CBF measurements with this technique [111], a particular important problem when studying patients with chronic cerebrovascular disease. Experience is limited, but expected and reproducible CBF changes are seen when the technique is applied, in conjunction with acetazolamide or CO2 manipulation, to healthy adults [111, 112], and those with cerebrovascular disease [113]. A study showed

that ASL MR imaging with acetazolamide challenge produced results comparable to those of ^{123}I-IMP SPECT in patients with arterial stenosis [114].

Blood oxygenation level-dependent MR imaging (BOLD)

BOLD imaging, used primarily for functional activation studies, has been applied to assess CA, despite the BOLD does not measure CBF directly. BOLD exploits the magnetic susceptibility differences between oxidative measures of regional oxygenation. The BOLD signal depends on several factors, including local CBF, cerebral blood volume, oxygen delivery, oxygen consumption, hemoglobin level, and pH [115]. BOLD signal has been shown also to change in response to CO2 alteration or acetazolamide challenge, although there is substantial variability in the response [116–118]. The same maneuvers that increase CBF generally result in an elevated regional relative proportion of oxy-hemoglobin. However, the effects of these challenge maneuvers in the setting of chronic flow impairment are not well established. Complex interplay exists between the physiological factors listed earlier, and BOLD signal will depend heavily on the degree and timing of theses changes. Limited studies demonstrated BOLD imaging response to vasodilatory challenge in patients with CA impairment [115, 118–120]. The response correlated moderately with SPECT response after acetazolamide [115], however, the response did not reliably match the TCD response [120].

Positron emission tomography (PET)

PET methods, which are used to assess CA, vary depending on the technique [121]. In general PET employs the juxtaposed measurement of CBF and oxygen extraction to determine whether perfusion pressure has fallen below levels where the oxygen demand of tissue can be met by changes in cerebrovascular resistance rather than measure the vascular response to a pharmacologic or physiologic challenge. Theoretically, an increased oxygen extraction fraction should correspond to the level where cerebrovascular resistance is depleted when assessed by a challenge test. In practice, however, it has been shown that these two measures are strongly related but not the same [93, 122]. Although oxygen extraction fraction has been chosen by some as the measure of choice for CA [123], it remains to be seen whether the oxygen extraction fraction or pharmacologic challenge of CA is superior in identifying patients at high risk of stroke.

In clinical practice, PET has disadvantages that currently limit its application. PET measurements require isotopes, chiefly ^{15}O, with a very short half-life; it therefore requires an on-site cyclotron. The availability of this equipment is limited. PET studies of the reserve are cumbersome and expensive, thus they are used more in clinical research than in routine practice. The spatial resolution of PET has improved substantially, but the studies still require long acquisition times and are sensitive to patient motion.

Single-photon emission CT (SPECT)

SPECT has been used in conjunction with several radiopharmaceutical agents to measure CBF and test cerebrovascular resistance [124]. These agents include technetium-99m-hexamethyl-propylenamine oxime (^{99m}Tc-HMPAO), ^{99m}Tc-ethylene cysteine dimmer (^{99m}Tc-ECD), and N-isopropyl-[iodine-123]-iodoamphetamine (^{123}I-IMP). They are extracted by the brain in proportion to local CBF. They have a long half-life, measured in hours, which allows time separation of injection and imaging long enough to obtain high signal-to-^{6}noise images. The assessment of CA with these agents can be performed with both qualitative and quantitative CBF measurements. The qualitative methods are less expensive and more simply performed but only allow assessment of relative CBF (i.e. comparison of the two hemispheres or comparison of cerebral hemispheres with cerebellum). Although the presence of impaired CA can be detected by these methods [125, 126], the results vary substantially [127], and have compared unfavorably with quantitative methods of flow assessment [128, 129]. These results are probably due in part to the fact the qualitative assessment of CA does not permit direct detection of the "steal" phenomenon. A degree of quantitation has been achieved with ^{123}I-IMP using a single arterial blood sample [129, 130]. With this method, it has been shown that acetazolamide-induced CBF change measured with these agents correlates with quantitative CBF response [129].

SPECT, performed with these agents, has several disadvantages that limit its clinical use. The long half-life of the injected agents necessitates either a several-day delay between the pre- and postacetazolamide studies, the use of different radiopharmaceuticals, or the use of only a small tracer does for the pre-acetazolamide study; each of theses machinations introduces potential errors when the two studies are compared. Imaging time itself is long. The nominal spatial resolution of SPECT studies is inferior to that of the other imaging modalities, and co-registration with CT or MR imaging is needed when intrahemispheric variability in CA is observed.

SPECT has also been performed with xenon-133 (^{133}Xe), a rapidly diffusible, inert radiotracer that is delivered by inhalation [131]. This method produces a quantitative CBF measurements [132, 133]. Although it is free of some of the difficulties of the injectable SPECT agents, the imaging times are long, and the spatial resolution is even less than that achieved with the other agents. Furthermore, the substantial attenuation of the low-energy gamma article emitted degrades the imaging of deep structures.

Xenon CT

Xenon CT also provides quantitative assessment of CBF and CA [90]. An approximately 70:30 mixture of oxygen and non-radioactive xenon gas is delivered by inhalation for several minutes, and serial CT scans are acquired. Because the X-ray attenuation of xenon exceeds that of cerebral tissue, the accumulation of this tracer can be measured over time. Using the Kety-Schmidt model, CBF can be delivered from this time course of oxygen accumulation over 5 to 6 minutes. This method provides reliable CBF quantitation [128] combined with high-resolution imaging methods [128, 134]. Although xenon inhalation at these concentrations is itself known to increase CBF after several minutes, the phenomenon has minimal effect with well-designed protocols [135]. The study can be performed before and after acetazolamide administration in the same session, because the xenon washes out of the brain rapidly.

These qualities make xenon CT well suited for assessment of CA, and this technique has received substantial clinical use and study. It has been validated against the "golden" standard mea-

sures of CBF [106] and correlates with PET-derived oxygen extraction fraction [136].

However, few centers have developed the expertise necessary to perform these studies successfully. Although xenon CT is usually well tolerated at the concentrations used for these studies, feelings of inebriation, somnolence, or dysphoria may occur and interfere with the study [135]. The technique is sensitive to head motion, and it can be difficult to maintain immobility for the duration of combined pre- and postacetazolamide imaging.

Clinical applications of autoregulation testing

Risk assessment of cerebral infarction

Autoregulatory response can predict stroke in some types of cerebrovascular disease. Patients with symptomatic occlusion of a major cerebral artery have eight times greater relative risk of cerebral infarction in the affected territory if they have evidence of diminished CA response [133, 137]. Some studies that included patients with severe stenosis have shown significantly increased incidence of cerebral infarction in those with impairment of CA [138–140].

Selection of patients for extracranial to intracranial bypass surgery

Despite a multicenter extra- to intracranial (EC-IC) bypass trial found no benefits from the procedure in patients with symptomatic stenosis or occlusion [141], it is likely that benefits can be achieved if selection was confined to patients with impaired CA and in whom thromboembolic infarction was excluded [123]. Several studies showed clinical benefits associated with improvement in CA response after surgery [96, 142–144].

Testing of CA in patients with Moya-moya disease appears to be particularly useful, because multiple severe proximal intracranial stenoses with subsequent extensive collateral circulation usually develop. Areas with impaired CA are at high risk of infarction, especially in children. Surgical revascularization procedures are often performed, after which dramatic improvement in CA response correlated with cessation of ischemic events has been demonstrated. The development of new vessels from the grafts occurs more reliably in areas of impaired CA, independent of local CBF, suggesting that impaired CA results in greater local angiogenic drive [145, 146]. Testing of CA is therefore likely to have an important role in selecting patients for revascularization and for the guidance of graft placement.

EC-IC bypass can also result in improved cognitive function in patients with impaired CA [147]. A large, randomized trial to assess effectiveness of EC-IC bypass in eligible patients with CA impairment as assessed using PET is under way [123].

Assessment of CA in conservative patients management

In patients with impaired CA the primary goal is to maintain adequate CPP, by optimization of cardiac function, minimizing orthostatic fluctuations of ABP, and limitations of antihypertensive medication. If CA is intact, emphasis may be placed instead on minimizing hypertension and avoiding thromboembolism. The relative merits of surgical and aggressive medical treatment for impaired CA, however, remain largely unstudied, as CA function can improve over time without surgical revascularization [137, 148]. In some patients temporizing with medical therapy for months to several years may allow the formation of sufficient collateral circulation to remove the risk of stroke from hypoperfusion.

Assessing risk of hyperperfusion syndrome

Hyperperfusion syndrome is a rare but disastrous complication of carotid endarterectomy. Hyperperfusion, defined as increased CBF after surgery, results in cerebral edema and intracerebral hemorrhage [149, 150]. The prognosis is poor, with mortality of 36% to 63%, and survivors have significant morbidity. If patients at risk for the syndrome can be identified preoperatively, strict control of ABP can be instituted in the early postoperative period [149, 151]. Assessment of CA can help to identify patients at risk for this phenomenon as postoperative hyperperfusion was seen only in patients with impaired CA (< 10% CBF response after acetazolamide) [152].

Balloon test occlusion

Balloon test occlusion of the internal carotid artery is performed to assess the adequacy of collateral circulation before permanent carotid artery occlusion. Most patients who tolerate 20 to 30 minutes of the occlusion without developing neurological deficits can safety undergo permanent occlusion [108]. However, approximately 10% of patients, who pass the clinical evaluation, suffer ipsilateral cerebral infarction after permanent occlusion. Several measures have been used to increase the sensitivity of balloon test occlusion, including pharmacologically induced hypotension, stump pressure measurements, and perfusion imaging; no consensus exists on the optimal protocol. Testing of CA has a strong theoretic advantage over mere CBF imaging for the same reasons that it provides superior evaluation in chronic cerebrovascular disease. Testing of CA with acetazolamide challenge has been performed during balloon test occlusion with promising results [108, 153].

References

1. Ito H, Kanno I, Kato C et al. Database of normal human cerebral blood flow, cerebral blood volume, cerebral oxygen extraction fraction and cerebral metabolic rate of oxygen measured by positron emission tomography with 15O-labelled carbon dioxide or water, carbon monoxide and oxygen: a multicentre study in Japan. Eur J Nucl Med Mol Imaging 2004; 31: 635–643.
2. Helenius J, Perkio J, Soinne L et al. Cerebral hemodynamics in a healthy population measured by dynamic susceptibility contrast MR imaging. Acta Radiol 2003; 44: 538–546.
3. Chih CP, Roberts Jr EL. Energy substrates for neurons during neural activity: a critical review of the astrocyte-neuron lactate shuttle hypothesis. J Cereb Blood Flow Metab 2003; 23: 1263–1281.
4. Baskurt OK, Meiselman HJ. Blood rheology and hemodynamics. Semin Thromb Hemost 2003; 29: 435–450.
5. McDonald DA. Arterial impedance. In: McDonald DA, editor. Blood flow in arteries. Williams & Willkins Co, Baltimore 1977: 351-389.
6. McDonald DA. The numerical analysis of cirulatory wave-forms. In: McDonald DA, editor. Blood flow in arteries. Williams&Wilkins Co, Baltimore 1974: 146–173.
7. Lassen NA. Cerebral blood flow and oxygen consumption in man. Physiol Rev 1959; 39: 183-238.
8. Strandgaard S, Olesen J, Skinhoj E, LASSEN NA. Autoregulation of

brain circulation in severe arterial hypertension. Br Med J 1973; 1: 507–510.
9. Waldemar G, Schmidt JF, Andersen AR, Vorstrup S, Ibsen H, Paulson OB. Angiotensin converting enzyme inhibition and cerebral blood flow autoregulation in normotensive and hypertensive man. J Hypertens 1989; 7: 229–235.
10. Wallis SJ, Firth J, Dunn WR. Pressure-induced myogenic responses in human isolated cerebral resistance arteries. Stroke 1996; 27: 2287––2290.
11. Garcia-Roldan JL, Bevan JA. Flow-induced constriction and dilation of cerebral resistance arteries. Circ Res 1990; 66: 1445–1448.
12. Thorin-Trescases N, Bevan JA. High levels of myogenic tone antagonize the dilator response to flow of small rabbit cerebral arteries. Stroke 1998; 29: 1194–1200.
13. McDonald DA. Blood flow in arteries. Williams & Willkins Co, Baltimore 1977.
14. Slish DF, Welsh DG, Brayden JE. Diacylglycerol and protein kinase C activate cation channels involved in myogenic tone. Am J Physiol Heart Circ Physiol 2002; 283: H2196–H2201.
15. Kitamura K, Xiong Z, Teramoto N, Kuriyama H. Roles of inositol trisphosphate and protein kinase C in the spontaneous outward current modulated by calcium release in rabbit portal vein. Pflugers Arch 1992; 421: 539–551.
16. McCarron JG, Crichton CA, Langton PD, MacKenzie A, Smith GL. Myogenic contraction by modulation of voltage-dependent calcium currents in isolated rat cerebral arteries. J Physiol 1997; 498 (Part 2): 371–379.
17. Ngai AC, Winn HR. Modulation of cerebral arteriolar diameter by intraluminal flow and pressure. Circ Res 1995; 77: 832–840.
18. Faraci FM. Role of nitric oxide in regulation of basilar artery tone in vivo. Am J Physiol 1990; 259: H1216–H1221.
19. Lee JE, Kwak J, Suh CK, Shin JH. Dual effects of nitric oxide on the large conductance calcium-activated potassium channels of rat brain. J Biochem Mol Biol 2006; 39: 91–96.
20. Miyahara K, Kawamoto T, Sase K et al. Cloning and structural characterization of the human endothelial nitric-oxide-synthase gene. Eur J Biochem 1994; 223: 719–726.
21. Kontos HA, Raper AJ, Patterson JL. Analysis of vasoactivity of local pH, PCO2 and bicarbonate on pial vessels. Stroke 1977; 8: 358–360.
22. Horiuchi T, Dietrich HH, Hongo K, Goto T, Dacey RG, Jr. Role of endothelial nitric oxide and smooth muscle potassium channels in cerebral arteriolar dilation in response to acidosis. Stroke 2002; 33: 844––849.
23. Kovecs K, Komjati K, Marton T, Skopal J, Sandor P, Nagy Z. Hypercapnia stimulates prostaglandin E(2) but not prostaglandin I(2) release in endothelial cells cultured from microvessels of human fetal brain. Brain Res Bull 2001; 54:387–390.
24. Lindauer U, Vogt J, Schuh-Hofer S, Dreier JP, Dirnagl U. Cerebrovascular vasodilation to extraluminal acidosis occurs via combined activation of ATP-sensitive and Ca^{2+}-activated potassium channels. J Cereb Blood Flow Metab 2003; 23: 1227–1238.
25. Toda N, Hatano Y, Mori K. Mechanisms underlying response to hypercapnia and bicarbonate of isolated dog cerebral arteries. Am J Physiol 1989; 257: H141–H146.
26. Simpson RE, Phillis JW. Adenosine deaminase reduces hypoxic and hypercapnic dilatation of rat pial arterioles: evidence for mediation by adenosine. Brain Res 1991; 553: 305–308.
27. Fredricks KT, Liu Y, Rusch NJ, Lombard JH. Role of endothelium and arterial K+ channels in mediating hypoxic dilation of middle cerebral arteries. Am J Physiol 1994; 267: H580–H586.
28. Horiuchi T, Dietrich HH, Hongo K, Dacey RG, Jr. Mechanism of extracellular K^+-induced local and conducted responses in cerebral penetrating arterioles. Stroke 2002; 33: 2692–2699.
29. Di Tullio MA, Tayebati SK, Amenta F. Identification of adenosine A1 and A3 receptor subtypes in rat pial and intracerebral arteries. Neurosci Lett 2004; 366: 48–52.
30. Kleppisch T, Nelson MT. Adenosine activates ATP-sensitive potassium channels in arterial myocytes via A2 receptors and cAMP--dependent protein kinase. Proc Natl Acad Sci USA 1995; 92: 12441––12445.
31. Li G, Cheung DW. Modulation of Ca(2+)-dependent K(+) currents in mesenteric arterial smooth muscle cells by adenosine. Eur J Pharmacol 2000; 394: 35–40.
32. Bleys RL, Cowen T. Innervation of cerebral blood vessels: morphology, plasticity, age-related, and Alzheimer's disease-related neurodegeneration. Microsc Res Tech 2001; 53: 106–118.
33. Baffi J, Gorcs T, Slowik F et al. Neuropeptides in the human superior cervical ganglion. Brain Res 1992; 570: 272–278.
34. Baumbach GL, Heistad DD. Effects of sympathetic stimulation and changes in arterial pressure on segmental resistance of cerebral vessels in rabbits and cats. Circ Res 1983; 52: 527–533.
35. Goadsby PJ, Uddman R, Edvinsson L. Cerebral vasodilatation in the cat involves nitric oxide from parasympathetic nerves. Brain Res 1996; 707: 110–118.
36. Hara H, Hamill GS, Jacobowitz DM. Origin of cholinergic nerves to the rat major cerebral arteries: coexistence with vasoactive intestinal polypeptide. Brain Res Bull 1985; 14: 179–188.
37. Morita-Tsuzuki Y, Hardebo JE, Bouskela E. Inhibition of nitric oxide synthase attenuates the cerebral blood flow response to stimulation of postganglionic parasympathetic nerves in the rat. J Cereb Blood Flow Metab 1993; 13: 993–997.
38. Edvinsson L, Ekman R, Jansen I, McCulloch J, Uddman R. Calcitonin gene-related peptide and cerebral blood vessels: distribution and vasomotor effects. J Cereb Blood Flow Metab 1987; 7: 720–728.
39. Edvinsson L, Brodin E, Jansen I, Uddman R. Neurokinin A in cerebral vessels: characterization, localization and effects in vitro. Regul Pept 1988; 20: 181–197.
40. Uddman R, Goadsby PJ, Jansen I, Edvinsson L. PACAP, a VIP-like peptide: immunohistochemical localization and effect upon cat pial arteries and cerebral blood flow. J Cereb Blood Flow Metab 1993; 13: 291–297.
41. Edvinsson L, Jansen O, I, Kingman TA, McCulloch J, Uddman R. Modification of vasoconstrictor responses in cerebral blood vessels by lesioning of the trigeminal nerve: possible involvement of CGRP. Cephalalgia 1995; 15: 373–383.
42. Lassen LH, Haderslev PA, Jacobsen VB, Iversen HK, Sperling B, Olesen J. CGRP may play a causative role in migraine. Cephalalgia 2002; 22: 54–61.
43. Weber JR, Angstwurm K, Bove GM et al. The trigeminal nerve and augmentation of regional cerebral blood flow during experimental bacterial meningitis. J Cereb Blood Flow Metab 1996; 16: 1319–1324.
44. Kalaria RN, Stockmeier CA, Harik SI. Brain microvessels are innervated by locus ceruleus noradrenergic neurons. Neurosci Lett 1989; 97: 203–208.
45. Moreno MJ, Lopez dP, Conde MV, Marco EJ. Cat cerebral arteries are functionally innervated by serotoninergic fibers from central and peripheral origins. Stroke 1995; 26: 271–275.
46. Sato A, Sato Y, Uchida S. Activation of the intracerebral cholinergic nerve fibers originating in the basal forebrain increases regional cerebral blood flow in the rat's cortex and hippocampus. Neurosci Lett 2004; 361: 90–93.
47. Cauli B, Tong XK, Rancillac A et al. Cortical GABA interneurons in neurovascular coupling: relays for subcortical vasoactive pathways. J Neurosci 2004; 24: 8940–8949.
48. Mulligan SJ, MacVicar BA. Calcium transients in astrocyte endfeet cause cerebrovascular constrictions. Nature 2004; 431: 195–199.

49. White RP, Hindley C, Bloomfield PM et al. The effect of the nitric oxide synthase inhibitor L-NMMA on basal CBF and vasoneuronal coupling in man: a PET study. J Cereb Blood Flow Metab 1999; 19: 673–678.
50. Belliveau JW, Kennedy DN, Jr., McKinstry RC et al. Functional mapping of the human visual cortex by magnetic resonance imaging. Science 1991; 254: 716–719.
51. Zonta M, Angulo MC, Gobbo S et al. Neuron-to-astrocyte signaling is central to the dynamic control of brain microcirculation. Nat Neurosci 2003; 6: 43–50.
52. Bezzi P, Carmignoto G, Pasti L et al. Prostaglandins stimulate calcium-dependent glutamate release in astrocytes. Nature 1998; 391: 281––285.
53. Bhardwaj A, Northington FJ, Carhuapoma JR et al. P-450 epoxygenase and NO synthase inhibitors reduce cerebral blood flow response to N-methyl-D-aspartate. Am J Physiol Heart Circ Physiol 2000; 279: H1616–H1624.
54. Gebremedhin D, Lange AR, Lowry TF et al. Production of 20-HETE and its role in autoregulation of cerebral blood flow. Circ Res 2000; 87: 60–65.
55. Christopherson KS, Hillier BJ, Lim WA, Bredt DS. PSD-95 assembles a ternary complex with the N-methyl-D-aspartic acid receptor and a bivalent neuronal NO synthase PDZ domain. J Biol Chem 1999; 274: 27467–27473.
56. Pelligrino DA, Gay RL, III, Baughman VL, Wang Q. NO synthase inhibition modulates NMDA-induced changes in cerebral blood flow and EEG activity. Am J Physiol 1996; 271: H990–H995.
57. Alonso-Galicia M, Drummond HA, Reddy KK, Falck JR, Roman RJ. Inhibition of 20-HETE production contributes to the vascular responses to nitric oxide. Hypertension 1997; 29:320–325.
58. Sun CW, Falck JR, Okamoto H, Harder DR, Roman RJ. Role of cGMP versus 20-HETE in the vasodilator response to nitric oxide in rat cerebral arteries. Am J Physiol Heart Circ Physiol 2000; 279: H339-H350.
59. Kara T, Narkiewicz K, Somers VK. Chemoreflexes — physiology and clinical implications. Acta Physiol Scand 2003; 177: 377–384.
60. Heistad DD, Marcus ML, Ehrhardt JC, Abboud FM. Effect of stimulation of carotid chemoreceptors on total and regional cerebral blood flow. Circ Res 1976; 38: 20–25.
61. Mitchell RA. Respiratory chemosensitivity in the medulla oblongata. J Physiol 1969; 202: 3P–4P.
62. Jordan J, Shannon JR, Diedrich A et al. Interaction of carbon dioxide and sympathetic nervous system activity in the regulation of cerebral perfusion in humans. Hypertension 2000; 36: 383–388.
63. Baumbach GL, Heistad DD. Effect of sympathetic stimulation and changes in arterial pressure on segmental resistance of cerebral vessels in rabitts and cats. Cir Res 1983; 52: 527–33.
63. Roatta S, Micieli G, Bosone D et al. Effect of generalised sympathetic activation by cold pressor test on cerebral haemodynamics in healthy humans. J Auton Nerv Syst 1998; 71: 159–166.
64. Heistad DD, Marcus ML. Total and regional cerebral blood flow during stimulation of carotid baroreceptors. Stroke 1976; 7: 239–243.
65. Rapela CE, Green HD, Denison AB, Jr. Baroreceptor reflexes and autorregulation of cerebral blood flow in the dog. Circ Res 1967; 21: 559–568.
66. Bondar RL, Kassam MS, Stein F, Dunphy PT, Fortney S, Riedesel ML. Simultaneous cerebrovascular and cardiovascular responses during presyncope. Stroke 1995; 26: 1794–1800.
67. Mokri B. The Monro-Kellie hypothesis - Applications in CSF volume depletion. Neurology 2001; 56: 1746–1748.
68. Miller JD. Intracranial pressure. Curr Opin Neurol Neurosurg 1989; 2: 15–20.
69. Kingman TA, Mendelow AD, Graham DI, Teasdale GM. Experimental intracerebral mass: time-related effects on local cerebral blood flow. J Neurosurg 1987; 67: 732–738.
70. Sahay KB, Mehrotra R, Sachdeva U, Banerji AK. Elastomechanical characterization of brain-tissues. Journal of Biomechanics 1992; 25: 319–26.
71. Johnston IH, Rowan JO. Raised intracranial pressure and cerebral blood flow. Venous outflow tract pressures and vascular resistances in experimental intracranial hypertension. J Neurol Neurosurg Psychiatry 1974; 37: 392–402.
72. Ikeyama A, Maeda S, Ito A, Banno K, Nagai H, Furuse M. The analysis of the intracranial pressure by the concept of the driving pressure from the vascular system. Neurochirurgia 1978; 21: 43–53.
73. Swiercz M, Mariak Z, Krejza J, Lewko J, Szydlik P. Intracranial pressure processing with artificial neural networks: prediction of ICP trends. Acta Neurochir (Wien) 2000; 142: 401–406.
74. Mariak Z, Swiercz M, Krejza J, Lewko J, Lyson T. Intracranial pressure processing with artificial neural networks: classification of signal properties. Acta Neurochir (Wien) 2000; 142: 407-411; discussion 411––412.
75. Ungerboeck K, Tenckhoff D, Heimann A, Wagner W, Kempski OS. Transcranial Doppler and cortical microcirculation at increased intracranial pressure and during the Cushing response: An experimental study on rabbits. Neurosurgery 1995; 36: 147–157.
76. Derdeyn CP, Grubb RL, Powers WJ. Cerebral hemodynamic impairment. Neurology 1999; 53: 251–259.
77. Powers WJ. Cerebral hemodynamics in ischemic cerebrovascular-disease. Ann Neurol 1991; 29: 231–240.
78. Rohl L, Ostergaard L, Simonsen CZ, Vestergaard-Poulsen P, Andersen G, Sakoh M et al. Viability thresholds of ischemic penumbra of hyperacute stroke defined by perfusion-weighted MRI and apparent diffusion coefficient. Stroke 2001; 32: 1140–1146.
79. Bassingt JB. Concurrent flow model for extraction during transcapillary passage. Circ Res 1974; 35: 483–503.
80. Tiecks FP, Lam AM, Aaslid R, Newell DW. Comparison of static and dynamic cerebral autoregulation measurements. Stroke 1995; 26: 1014–1019.
81. Aaslid R, Lash SR, Bardy GH, Gild WH, Newell DW. Dynamic pressure-flow velocity relationships in the human cerebral circulation. Stroke 2003; 34: 1645–1649.
82. Paulson OB, Strandgaard S, Edvinsson L. Cerebral autoregulation. Cerebrovasc Brain Metab Rev 1990; 2: 161–192.
83. Heuser D, Astrup J, Lassen NA, Betz E. Brain carbonic-acid acidosis after acetazolamide. Acta Physiol Scand 1975; 93: 385–390.
84. Vorstrup S, Henriksen L, Paulson OB. Effect of acetazolamide on cerebral blood-flow and cerebral metabolic-rate for oxygen. J Clin Invest 1984; 74: 1634–1639.
85. Okazawa H, Yamauchi H, Sugimoto K, Toyoda H, Kishibe Y, Takahashi M. Effects of acetazolamide on cerebral blood flow, blood volume, and oxygen metabolism: A positron emission tomography study with healthy volunteers. J Cereb Blood Flow Metab 2001; 21: 1472–1479.
86. Sorteberg W, Lindegaard KF, Rootwelt K et al. Effect of acetazolamide on cerebral-artery blood velocity and regional cerebral blood-flow in normal subjects. Acta Neurochir 1989; 97: 139–145.
87. Grossmann WM, Koeberle B. The dose-response relationship of acetazolamide on the cerebral blood flow in normal subjects. Cerebrovasc Dis 2000; 10: 65–69.
88. Sullivan HG, Kingsbury TB, Morgan ME et al. The rCBF response to diamox in normal subjects and cerebrovascular-disease patients. J Neurosurg 1987; 67: 525–534.
89. Kuwabara Y, Ichiya Y, Sasaki M, Yoshida T, Masuda K. Time dependency of the acetazolamide effect on cerebral hemodynamics in patients with chronic occlusive cerebral-arteries — early steal phenomenon demonstrated by [O-15]H2O positron emission tomography. Stroke 1995; 26: 1825–1829.

90. Yonas H, Pindzola RR. Physiological determination of cerebrovascular reserves and its use in clinical management. Cerebrovasc Brain Metab Rev 1994; 6: 325–340.
91. Petrella JR, Decarli C, Dagli M et al. Age-related vasodilatory response to acetazolamide challenge in healthy adults: A dynamic contrast-enhanced MR study. Am J Neurorad 1998; 19: 39–44.
92. Brian JE. Carbon dioxide and the cerebral circulation. Anesthesiology 1998; 88: 1365–1386.
93. Kanno I, Uemura K, Higano S et al. Oxygen extraction fraction at maximally vasodilated tissue in the ischemic brain estimated from the regional co2 responsiveness measured by Positron Emission Tomography. J Cereb Blood Flow Metab 1988; 8: 227–235.
94. Kazumata K, Tanaka N, Ishikawa T, Kuroda S, Houkin K, Mitsumori K. Dissociation of vasoreactivity to acetazolamide and hypercapnia — Comparative study in patients with chronic occlusive major cerebral artery disease. Stroke 1996; 27: 2052–2058.
95. Gambhir S, Inao S, Tadokoro M, Nishino M, Ito K, Ishigaki T et al. Comparison of vasodilatory effect of carbon dioxide inhalation and intravenous acetazolamide on brain vasculature using positron emission tomography. Neurol Res 1997; 19: 139–144.
96. Ringelstein EB, Vaneyck S, Mertens I. Evaluation of cerebral vasomotor reactivity by various vasodilating stimuli — comparison of CO2 to acetazolamide. J Cereb Blood Flow Metab 1992; 12: 162-168.
97. Vorstrup S, Lassen NA. Evaluation of the cerebral vasodilatory capacity before extracranial-intracranial bypass-surgery. Acta Neurol Scand 1986; 73: 538.
98. Lam JM, Hsiang JN, Poon WS. Monitoring of autoregulation using laser Doppler flowmetry in patients with head injury. J Neurosurg 1997; 86: 438–445.
99. Bouma GJ, Muizelaar JP. Relationship between cardiac output and cerebral blood flow in patients with intact and with impaired autoregulation. J Neurosurg 1990; 73: 368–374.
100. Aaslid R, Lindegaard KF, Sorteberg W, Nornes H. Cerebral autoregulation dynamics in humans. Stroke 1989; 20: 45–52.
101. Tiecks FP, Douville C, Byrd S, Lam AM, Newell DW. Evaluation of impaired cerebral autoregulation by the Valsalva maneuver. Stroke 1996; 27: 1177–1182.
102. Brauer P, Kochs E, Werner C, Bloom M, Policare R, Pentheny S et al. Correlation of transcranial Doppler sonography mean flow velocity with cerebral blood flow in patients with intracranial pathology. J Neurosurg Anesthesiol 1998; 10: 80–85.
103. Demolis P, Dinh YRT, Giudicelli JF. Relationships between cerebral regional blood flow velocities and volumetric blood flows and their respective reactivities to acetazolamide. Stroke 1996; 27: 1835–1839.
104. Krejza J, Swiat M, Pawlak M et al. Suitability of temporal bone acoustic window: conventional TCD versus transcranial color-coded duplex sonography. J Neuroimaging 2007 (in press).
105. Ostergaard L, Weisskoff RM, Chesler DA, Gyldensted C, Rosen BR. High resolution measurement of cerebral blood flow using intravascular tracer bolus passages. 1. Mathematical approach and statistical analysis. Magn Reson Med 1996; 36: 715–725.
106. Latchaw RE, Yonas H, Hunter GJ et al. Guidelines and recommendations for perfusion imaging in cerebral ischemia — A Scientific Statement for Healthcare Professionals by the Writing Group on Perfusion Imaging, from the Council on Cardiovascular Radiology of the American Heart Association. Stroke 2003; 34: 1084–1104.
107. Eastwood JD, Alexander MJ, Petrella JR, Provenzale JM. Dynamic CT perfusion imaging with acetazolamide challenge for the preprocedural evaluation of a patient with symptomatic middle cerebral artery occlusive disease. Am J Neuroradiol 2002; 23: 285–297.
108. Jain R, Hoeffner EG, Deveikis JP, Harrigan MR, Thompson BG, Mukherji SK. Carotid perfusion CT with balloon occlusion and acetazolamide challenge test: Feasibility. Radiology 2004; 231: 906–913.
109. Guckel FJ, Brix G, Schmiedek P et al. Cerebrovascular reserve capacity in patients with occlusive cerebrovascular disease: Assessment with dynamic susceptibility contrast-enhanced MR imaging and the acetazolamide stimulation test. Radiology 1996; 201: 405–412.
110. Schreiber WG, Guckel F, Stritzke P, Schmiedek P, Schwartz A, Brix G. Cerebral blood flow and cerebrovascular reserve capacity: Estimation by dynamic magnetic resonance imaging. J Cereb Blood Flow Metab 1998; 18: 1143–1156.
111. Yen YF, Field AS, Martin EM et al. Test-retest reproducibility of quantitative CBF measurements using FAIR perfusion MRI and acetazolamide challenge. Magn Reson Med 2002; 47: 921–928.
112. Kastrup A, Li TQ, Glover GH, Moseley ME. Cerebral blood flow-related signal changes during breath-holding. Am J Neurorad1999; 20: 1233–1238.
113. Detre JA, Alsop DC. Perfusion magnetic resonance imaging with continuous arterial spin labeling: methods and clinical applications in the central nervous system. Eur J Radiol 1999; 30: 115–124.
114. Arbab AS, Aoki S, Toyama K et al. Quantitative measurement of regional cerebral blood flow with flow-sensitive alternating inversion recovery imaging: Comparison with [iodine123]-iodoamphetamin single photon emission CT. Am J Neurorad 2002; 23: 381–388.
115. Shiino A, Morita Y, Tsuji A et al. Estimation of cerebral perfusion reserve by blood oxygenation level-dependent imaging: Comparison with single-photon emission computed tomography. J Cereb Blood Flow Metab 2003; 23: 121–135.
116. Rostrup E, Larsson HBW, Toft PB et al. Functional MRI of CO2 induced increase in cerebral perfusion. NMR Biomed 1994; 7: 29–34.
117. Hedera P, Lai S, Lewin JS et al. Assessment of cerebral blood flow reserve using functional magnetic resonance imaging. J Magn Reson Imag 1996; 6: 718–725.
118. Bruhn H, Kleinschmidt A, Boecker H. The effect of acetazolamide on regional cerebral blood oxygenation at rest and under stimulation as assessed by MRI. J Cereb Blood Flow Metab 1994; 14: 742–748.
119. Kleinschmidt A, Steinmetz H, Sitzer M, Merboldt KD, Frahm J. Magnetic-resonance-imaging of regional cerebral blood oxygenation changes under acetazolamide in carotid occlusive disease. Stroke 1995; 26: 106–110.
120. Lythgoe DJ, Williams SCR, Cullinane M, Markus HS. Mapping of cerebrovascular reactivity using bold magnetic resonance imaging. Magn Reson Imag 1999; 17: 495–502.
121. Baron JC, Frackowiak RS, Herholz K et al. Use of PET methods for measurement of cerebral energy metabolism and hemodynamics in cerebrovascular disease. J Cereb Blood Flow Metab 1989; 9: 723––742.
122. Nemoto EM, Yonas H, Kuwabara H et al. Identification of Hemodynamic compromise by cerebrovascular reserve and oxygen extraction fraction in occlusive vascular disease. J Cereb Blood Flow Metab 2004; 24: 1081–1089.
123. Adams HP, Jr., Powers WJ, Grubb RL, Jr., Clarke WR, Woolson RF. Preview of a new trial of extracranial-to-intracranial arterial anastomosis: the carotid occlusion surgery study. Neurosurg Clin N Am 2001; 12: 613–661.
124. Catafau AM. Brain SPECT in clinical practice. Part 1: Perfusion. J Nucl Med 2001; 42: 259–271.
125. Hirano T, Minematsu K, Hasegawa Y, Tanaka Y, Hayashida K, Yamaguchi T. Acetazolamide reactivity on I-123 Imp single-photon emission computed-tomography in patients with major cerebral-artery occlusive disease - correlation with positron emission tomography parameters. J Cereb Blood Flow Metab 1994; 14: 763–770.
126. Imaizumi M, Kitagawa K, Hashikawa K et al. Detection of misery perfusion with split-dose I-123-iodoamphetamine single-photon emission computed tomography in patients with carotid occlusive diseases. Stroke 2002; 33: 2217–2223.

127. Yokota C, Hasegawa Y, Minematsu K, Yamaguchi T. Effect of acetazolamide reactivity and long-term outcome in patients with major cerebral artery occlusive diseases. Stroke 1998; 29: 640–644.
128. Yonas H, Pindzola RR, Meltzer CC, Sasser H. Qualitative versus quantitative assessment of cerebrovascular reserves. Neurosurgery 1998; 42: 1005–1010.
129. Ogasawara K, Ito H, Sasoh M et al. Quantitative measurement of regional cerebrovascular reactivity to acetazolamide using (123) I-N--isopropyl-p-iodoamphetamine autoradiography with SPECT: Validation study using (H2O)-O-15 with PET. J Nucl Med 2003; 44: 520––525.
130. Ogasawara K, Okuguchi T, Sasoh M et al. Qualitative versus quantitative assessment of cerebrovascular reactivity to acetazolamide using iodine-123-N-isopropyl-p-iodoamphetamine SPECT in patients with unilateral major cerebral artery occlusive disease. AJNR Am J Neuroradiol 2003; 24: 1090–1095.
131. Lassen NA, Henriksen L, Paulson O. Regional cerebral blood-flow in stroke by Xe-133 inhalation and emission tomography. Stroke 1981; 12: 284–288.
132. Payne JK, Trivedi MH, Devous MD. Comparison of technetium-99m--HMPAO and xenon-133 measurements of regional cerebral blood flow by SPECT. J Nucl Med 1996; 37: 1735–1740.
133. Ogasawara K, Ogawa A, Terasaki K, Shimizu H, Tominaga T, Yoshimoto T. Use of cerebrovascular reactivity in patients with symptomatic major cerebral artery occlusion to predict 5-year outcome: Comparison of xenon-133 and iodine-123-IMP single-photon emission computed tomography. J Cereb Blood Flow Metab 2002; 22: 1142–1148.
134. Yonas H, Darby JM, Marks EC, Durham SR, Maxwell C. CBF measured by Xe-CT: approach to analysis and normal values. J Cereb Blood Flow Metab 1991; 11: 716–725.
135. Witt JP, Holl K, Heissler HE, Dietz H. Stable Xenon Ct Cbf — effects of blood-flow alterations on Cbf calculations during inhalation of 33-percent stable Xenon. AJNR Am J Neuroradiol 1991; 12: 973–975.
136. Nariai T, Suzuki R, Hirakawa K, Maehara T, Ishii K, Senda M. Vascular reserve in chronic cerebral-ischemia measured by the acetazolamide challenge test - comparison with positron emission tomography. AJNR Am J Neuroradiol 1995; 16: 563–570.
137. Kuroda S, Houkin K, Kamiyama H, Mitsumori K, Iwasaki Y, Abe H. Long-term prognosis of medically treated patients with internal carotid or middle cerebral artery occlusion — Can acetazolamide test predict it? Stroke 2001; 32: 2110–2115.
138. Kleiser B, Widder B. Course of carotid artery occlusions with impaired cerebrovascular reactivity. Stroke 1992; 23: 171–174.
139. Vernieri F, Pasqualetti P, Passarelli F, Rossini PM, Silvestrini M. Outcome of carotid artery occlusion is predicted by cerebrovascular reactivity. Stroke 1999; 30: 593–8.
140. Settakis G, Molnar C, Kerenyi L et al. Acetazolamide as a vasodilatory stimulus in cerebrovascular diseases and in conditions affecting the cerebral vasculature. Eur J Neurol 2003; 10: 609–620.
141. Barnett HJM. Failure of extracranial intracranial arterial bypass to reduce the risk of ischemic stroke — results of an international randomized trial. NEJM 1985; 313: 1191–200.
142. Karnik R, Valentin A, Ammerer HP, Donath P, Slany J. Evaluation of vasomotor reactivity by transcranial Doppler and acetazolamide test before and after extracranial-intracranial bypass in patients with internal carotid artery occlusion. Stroke 1992; 23: 812–817.
143. Kuroda S, Kamiyama H, Abe H et al. Acetazolamide test in detecting reduced cerebral perfusion reserve and predicting long-term prognosis in patients with internal carotid-artery occlusion. Neurosurgery 1993; 32: 912–919.
144. Schmiedek P, Piepgras A, Leinsinger G, Kirsch CM, Einhaupl K. Improvement of cerebrovascular reserve capacity by EC-IC arterial bypass-surgery in patients with ICA occlusion and hemodynamic cerebral-ischemia. J Neurosurg 1994; 81: 236–244.
145. Nariai T, Suzuki R, Matsushima Y et al. Surgically induced angiogenesis to compensate for hemodynamic cerebral-ischemia. Stroke 1994; 25: 1014–1021.
146. Iwama T, Hashimoto N, Takagi Y, Tsukahara T, Hayashida K. Predictability of extracranial/intracranial bypass function: A retrospective study of patients with occlusive cerebrovascular disease. Neurosurgery 1997; 40: 53–59.
147. Sasoh M, Ogasawara K, Kuroda K et al. Effects of EC-IC bypass surgery on cognitive impairment in patients with hemodynamic cerebral ischemia. Surg Neurol 2003; 59: 455–460.
148. Widder B, Kleiser B, Krapf H. Course of cerebrovascular reactivity in patients with carotid-artery occlusions. Stroke 1994; 25: 1963–1977.
149. Henderson RD, Phan TG, Piepgras DG, Wijdicks EFM. Mechanisms of intracerebral hemorrhage after carotid endarterectomy. J Neurosurg 2001; 95: 964–979.
150. Piepgras DG, Morgan MK, Sundt TM, Yanagihara T, Mussman LM. Intracerebral hemorrhage after carotid endarterectomy. J Neurosurg 1988; 68: 532–536.
151. Reigel M, Hollier LH, Kazmier FJ, Obrien PC. Hypertension and late survival in aneurysm patients. J Am Coll Cardiol 1987; 9: A114.
152. Hosoda K, Kawaguchi T, Ishii K et al. Prediction of hyperperfusion after carotid endarterectomy by brain SPECT analysis with semiquantitative statistical mapping method. Stroke 2003; 34: 1187–1193.
153. Okudaira Y, Arai H, Sato K. Cerebral blood flow alteration by acetazolamide during carotid balloon occlusion — parameters reflecting cerebral perfusion pressure in the acetazolamide test. Stroke 1996; 27: 617–621.